Asian Journal of Chemistry; Vol. 25, No. 18 (2013), 10425-10430

ASIAN JOURNAL OF CHEMISTRY

http://dx.doi.org/10.14233/ajchem.2013.15628

Optimization of Evodiamine-Imprinted Composite Membrane by Orthogonal Design Method

HUILING CHENG[1], GUANGYAN HE[1], XIUFANG ZHU[1], HAO ZHOU[1], MINGFENG WANG[2], QIUE CAO[1] and ZHONGTAO DING[†,*]

[1]Key Laboratory of Medicinal Chemistry for Nature Resource, Ministry of Education; School of Chemical Science and Technology, Yunnan University, Kunming 650091, Yunnan Province, P.R. China
[2]Technology Center, Hongyun-Honghe Tobacco (Group) Co. Ltd., Kunming 650202, Yunnan Province, P.R. China

*Corresponding author: Tel/Fax: +86 871 65033910; E-mail: ztding@ynu.edu.cn; ynchenghl@163.com

(*Received*: 12 April 2013; *Accepted*: 20 November 2013) AJC-14418

In the study, a series of molecularly imprinted composite membranes (MICMs) for evodiamine were prepared by orthogonal experiment design involving four factors, each at three levels. The results indicated that the imprinted membrane derived from commercial cellulose acetate and nylon microfiltration membranes in tetrahydrofuran yielded the highest imprinting factor of 3.099. Characterization results by scanning electron microscopy and N_2 adsorption analysis showed that the optimized imprinted membrane ($MICM_{opt}$) possessed different pore structure and surface morphology from the non-imprinted membrane ($NICM_{opt}$). Under the drive of concentration difference, $MICM_{opt}$ can preferably transfer evodiamine and its transfer mechanism conforms to the "gate effect" mechanism. As a result of imprinting effect, $MICM_{opt}$ can enrich evodiamine from the crude extraction of the herb *Evodia rutaecarpa* with a concentration effect (1.72 times). The results show a promising application potential of $MICM_{opt}$ in the separation and enrichment of evodiamine in the complex system.

Key Words: Molecularly imprinted membrane, Evodiamine, Optimization, Orthogonal design method, Surface modification.

INTRODUCTION

The plant species *Evodia rutaecarpa* is a Chinese herb used in the treatment of gastrointestinal disorders and headache[1]. Evodiamine (EVO), a major quinazolinocarbolic alkaloid isolated from the fruit of *E. rutaecarpa*, has been proven to have antipolysarcous, analgesic, anticancer and bronchoconstrictive activities and is now widely used in clinical therapy[2,3]. With the growing demands of EVO, its preparation became a hot spot in EVO research field. However, extracting EVO from the natural plants is always time-consuming and ineffective due to the poor affinity and selectivity of conventional separation materials. Therefore, it is essential to develop an effective separation material with high affinity and selectivity to evodiamine.

As a potential separation material, membrane is thought to be a likely choice for the purification of EVO, if properly modified. Currently, membrane separation is indispensable in a great number of modern applications, such as the production of drinking water, pharmaceutical and medicine manufacture[4]. However, traditional membranes suffer from the lack of specific selectivity toward target molecules against their analogues with similar molecular weight and volume, which greatly limits its application in a variety of fields. Surface modification is a convenient way to solve this problem.

Molecular imprinting has been verified to be the most facile technique to introduce molecular recognition sites into a commercial membrane[5]. By coating a layer of functional polymers on the walls of pores in commercial membranes, it is possible to enhance the selectivity, permeability or to introduce other desirable properties for the membranes. A molecularly imprinted composite membrane (MICM) can combine the inherent features of base membrane with the introduced properties of the molecularly imprinted polymers. As one hot subject in the membrane separation field, MICM has been used in various applications, such as chiral separation, solid-phase extraction, herbicides detection, biosensor, *etc.*[6].

Basically, a commercial membrane is mainly used as the support for functional polymer, while the intelligent polymer coating on the supporting membrane is the main recognition component of MICM. It is obvious that the polymer plays a key role for the selectivity of MICM[7]. On the other hand, recent studies have revealed that the surface properties of a support membrane and soaking-time in a reaction system also affect the morphology and thickness of coating layers[8]. Therefore, imprinting process on a membrane is very complicated and influenced by many factors including the types and amounts of functional monomer and cross-linker, solvent, initiator, supporting membrane, *etc*. Since it is difficult to

optimize molecularly imprinted membrane by traditional single-factor experimental method, orthogonal design was used to determine the factors and parameters for the imprinting process in present study. Orthogonal design is one important statistical method that includes the Taguchi parameter design methodology[9]. By using this method, it is possible to evaluate the effects of many factors with relatively low cost and reduced number of experiments. Up to now, orthogonal experimental design has been successfully applied in chemistry and chemical engineering for the process parameter optimization[10].

In this paper, a series of MICMs selective to EVO was prepared by orthogonal experimental method. Four factors including the type of support membrane, the amount of cross-linker, the type of solvent and soaking-time duration were considered in the experimental design. The selectivity of various MICMs was evaluated by comparing their equilibrium binding amounts with those of the control non-imprinted composite membranes (NICMs). The structure of optimal MICM ($MICM_{opt}$) was characterized by scanning electron microscopy (SEM) and N_2 sorption analysis. Competitive permeability of $MICM_{opt}$ to EVO was then studied under the drive of concentration difference. As expected, $MICM_{opt}$ yielded a satisfactory effect on EVO enrichment. To our best of knowledge, this is the first report of the molecularly imprinted membrane tailored to evodiamine.

EXPERIMENTAL

Evodiamine (EVO) and rutaecarpine (RUT) were purchased from Anli Chemical Corporation (Tianjing, China). Their structures are shown in Fig. 1. *E. rutaecarpa* was purchased from Fulintang Pharmaceuticals (Kunming, China). Three microfiltration membranes, namely polyvinylidene fluoride (PVDF), nylon (Nylon) and cellulose acetate membrane (CA), with identical nominal pore sizes of 0.45 μm and thicknesses of 125 μm were all purchased from Shanghai Yadong Heji Rosin Co. Ltd. (Shanghai, China). Methacrylic acid (MAA) and ethylene glycol dimethacrylate (EDMA) were purchased from Suzhou Anli Chemical Plant (Jiangsu, China) and were distilled under vacuum to remove stabilizers prior to use. Azobisisobutyronitrile (AIBN) was the product of Shanghai Fourth Reagent Plant (Shanghai, China), recrystallized from ethanol before use. All solvents were analytical or HPLC-grade and used without further purification.

Chromatographic evaluation was carried out on a Waters High Performance Liquid Chromatography system (HPLC, USA) equipped with Waters-1525 pump, Waters 2996 UV/VIS detector and Waters-717 automatic injector model. The analytical column was a Waters C_{18} column (250 mm × 4.6 mm i.d.; 5 μm). The flow rate was kept at 1 mL min^{-1}. The mobile phase was composed of A (2 % v/v THF in MeCN) and B (0.2 % v/v aqueous solution of ammonium acetate) with a ratio of 1:1 (v/v). The detection wavelength was 280 nm. The column was maintained at 25 ºC. Under these conditions, EVO and RUT in MeOH can be isolated from other interfering components in the range of 0.05-0.50 mg mL^{-1} with the calibration curve expressed as A = -89035.1 + 665170.35C (R = 0.9999, RSD = 0.18 %) for EVO and A = -125881.05 + 103180.0C (R = 0.9999, RSD = 0.32 %) for RUT, where A and C are the peak area and concentration of the substrate, respectively.

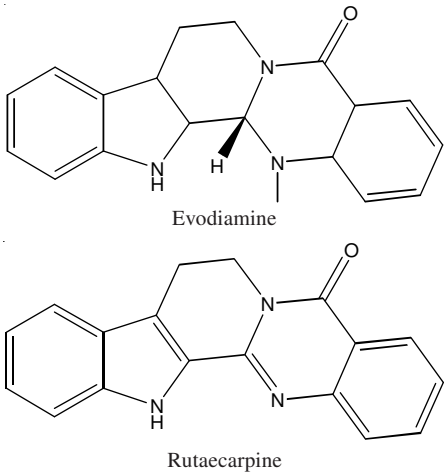

Fig. 1. Molecular structures of evodiamine and rutaecarpine. Evodiamine is the template molecule evodiamine and rutaecarpine is the analogue rutaecarpine

A UV-2401 double-beam spectrophotometer (Shimadzu, Japan) was used to determine the UV spectra of EVO. A HZ constant temperature bath oscillator (Jiangsu, China) was utilized in binding experiments. An H-shape permeation device (Tianjin, China) was used to explore the permeating flux and permeation selectivity of the polymer membranes. The surface morphology and the cross-section structure of the membranes were observed by a Hitachi S-520 field emission scanning electron microscope (Tokyo, Japan). The N_2 adsorption/desorption analysis was done by a NOVA 2000e gas sorption analyzer (Quantachrome Corp., USA).

Preparation of membranes: A series of EVO imprinted membranes, labeled as $MICM_1$, $MICM_2$, … $MICM_9$, were prepared according to the orthogonal design table of L_9 (3^4) (Table-1). A typical process for $MICM_{1-6}$ preparation was begun with dissolving EVO (0.20 mmol) and MAA (0.80 mmol) in THF (or $CHCl_3$, MeOH, 3.5 mL). After shaking for 3 h, the cross-linking agent EDMA and the initiator AIBN (0.5 % of the total moles of EDMA and MAA) were added according to Table-1. The imprinting solution was ultrasonically degassed for 5 min and then a circular PVDF or Nylon membrane (area: 2.25 cm^2) was immersed in the solution. After a necessary time, the membrane was taken out and mounted between two pieces of glass, then sealed and heated at 60 ºC for 24 h. The membrane was placed in a Soxhlet apparatus and washed with 10 % (v/v) AcOH/MeOH until no EVO in the eluate could be detected at 240 nm. Finally, the membrane was rinsed with MeOH to remove residual AcOH and dried to constant weight under vacuum.

By comparison, the preparation of $MICM_{7-9}$ was more elaborated. At first, a CA membrane was uniformly dispersed in the degassed THF solution. Then a nylon membrane was soaked in this solution for a period of time and the composite membrane of Nylon modified by CA (CA-Nylon) was obtained. The subsequent polymerization was carried out on this CA-nylon membrane.

Correspondingly, the control non-imprinted membranes ($NICM_{1-9}$) were also prepared simultaneously in the absence of the template (EVO) and treated by the same procedure as MICM.

TABLE-1
ORTHOGONAL DESIGN SYNTHESIS OF IMPRINTED MEMBRANES

Imprinted membrane	Solvent	Supporting membrane	Dosage of cross-linker (mL)	Soaking-time (s)
$MICM_1$	$CHCl_3$	PVDF	0.15	30
$MICM_2$	MeOH	PVDF	0.30	180
$MICM_3$	THF	PVDF	0.75	1800
$MICM_4$	$CHCl_3$	Nylon	0.30	1800
$MICM_5$	MeOH	Nylon	0.75	30
$MICM_6$	THF	Nylon	0.15	180
$MICM_7$	$CHCl_3$	CA-Nylon	0.75	180
$MICM_8$	MeOH	CA-Nylon	0.15	1800
$MICM_9$	THF	CA-Nylon	0.30	30

Equilibrium binding experiments: The imprinted membrane or control non-imprinted membrane (20 mg each) was placed in a 25 mL Erlenmeyer flask and mixed with 10 mL of EVO solution (0.40 mmol l^{-1}), respectively. The mixture was oscillated at 25 ºC for 12 h. The concentration of free substrate in the solution was determined at 240 nm by UV spectrometry. The adsorption capacity (Q), which was defined as the amount of substrate (μmol) binding to 1 g of polymer membrane, was calculated by subtracting the concentration of free substrate from its initial concentration. The average values of triplicate independent results were obtained.

Preparation of sample solution: The powder of *E. rutaecarpa* (7.0 g) was extracted with 70 mL of MeOH for 2 h in a Soxhlet apparatus. The procedure was repeated three times and the filtrates were mixed together and evaporated under reduced pressure. Finally, the extract was redissolved in 250 mL of MeOH to obtain the sample solution.

Permeation experiment: Selective transportation of substrates was measured using an H-shape permeation device with two-compartment membrane cells, (70 mL, each). A membrane was fitted tightly at the connecting joint between two cells. The cells were well designed so that the area available for diffusion was about 1.13 cm^2. In the left cell, 60 mL of EVO/RUT mixture (0.10 mmol L^{-1} each in MeOH) or real herb samples were added, while the right cell was filled with the pure solvent (60 mL). The solution in each cell was stirred by a mechanical stirrer at a constant speed. The substrate penetrating through the membrane was measured by calculating the concentration of the removal (200 μL) from the sample solution in the left cell with an interval of 1 h in the range of 0-12 h. The concentration of substrate was analyzed by HPLC based on the established calibration curves. The penetrating amounts were defined as the mass of EVO (mg) per area of membrane barrier (cm^2). After each sampling, 200 μL of fresh solvent was added to maintain the volume of solution in the left cell at 60 mL.

RESULTS AND DISCUSSION

Optimization of imprinting composite membranes by orthogonal design

Choice of factors and levels: In this study, a molecularly imprinted composite membrane (MICM) was prepared by the copolymerization of functional monomer and cross-linker in the presence of template on all surfaces in the internal pores of a porous membrane. Although the supporting membrane is mainly used as the support of functional polymer, its surface properties (phobility/phibility) and soaking-time in a reaction solution may affect the morphology and thickness of polymer sediment layers[11]. On the other hand, as the main recognition component of MICM, the smart polymer coating on the supporting membrane is vital for its recognition ability and the conditions for its preparation must be optimized. Previous studies revealed that the functional monomer acts as the bridge to bring template molecules into polymer materials and its type and amount determine the selectivity of MICM[12]. It is also reported that the cross-linking agent constitutes the matrix structure and regulates the pore's morphology of polymers and transfer rate[13]. In addition, the polarity of porogen can affect the strength of host-guest complex and mediate the direction of extension of polymer chains[7]. According to our preliminary study, methacrylic acid (MAA) is an appropriate functional monomer in EVO imprinting system. Therefore, MAA was selected in the study and the EVO/MAA ratio was fixed at an established mole ratio of 1:4. Therefore, in this study, the four factors and their levels were set as follows: (i) supporting membrane (PVDF, Nylon, CA-Nylon); (ii) the amount of cross-linker (0.15, 0.30, 0.75 mL); (iii) solvent ($CHCl_3$, MeOH, THF); and (iv) soaking-time (30, 180, 1800 s). Nine imprinted and non-imprinted membranes were prepared according to a standardized orthogonal table $L_9(3^4)$ (Table-1).

Analysis of results: Table-2 indicates the binding amounts (Q) of EVO on various MICMs and the control NICMs measured by equilibrium binding experiments. The imprinting factor (α), defined as the ratio of binding amounts of MICM to the control NICM ($\alpha = Q_{MICM}/Q_{NICM}$), was used as the assessment indicator in variance analysis. According to the literature[14], the accumulated effects of the factors ($K = \Sigma\alpha$) at three levels were calculated respectively. Range (R) was used to evaluated the superiority and inferiority for factors, where $R = K_{max}-K_{min}$. The results of variance analysis are shown in Table-3.

TABLE-2
BINDING AMOUNTS OF MEMBRANES (Q)[a]

Membrane	Q_{MICM} (μmol g^{-1})	Q_{NICM} (μmol g^{-1})	$\alpha = Q_{MICM}/Q_{NICM}$
$MICM_1$	18.90	38.39	0.492
$MICM_2$	26.09	27.98	0.932
$MICM_3$	21.74	23.78	0.914
$MICM_4$	6.31	14.19	0.445
$MICM_5$	17.84	17.97	0.993
$MICM_6$	17.71	15.13	1.171
$MICM_7$	39.70	15.24	2.605
$MICM_8$	23.45	21.04	1.115
$MICM_9$	46.74	15.45	3.025

[a]Binding amounts were determined by adding 4.0 μmol of EVO in solvent (10 ml) to 20.0 mg of polymer membranes.

According to the R values shown in Table-3, the type of supporting membrane was the dominant factor among the imprinting factors and the self-made CA-nylon composite membrane yielded the highest imprinting effect. The second significant factor was the dosage of cross-linking agent. Compared with the other levels, 0.75 mL of cross-linker (EDMA) could consolidate more MAA-EVO complexes into the intelligent polymers, leading to the highest selectivity. The influence of

TABLE-3
RESULTS OF VARIANCE ANALYSIS

	Solvent	Supporting membrane	Dosage of cross-linker (mL)	Soaking-time (s)
K_1	3.542	2.339	2.777	4.510
K_2	3.040	2.608	4.402	4.708
K_3	5.110	6.745	4.512	2.473
R	2.070	4.406	1.735	2.235
Optimum level	THF	CA-Nylon	0.75	180

solvent and the soaking-time is relatively weak and too long soaking time (over 180 s) did not facilitate the improvement of imprinting efficiency. Therefore, the optimal conditions were established and listed in the order from the most to the least important as follows: supporting membrane (CA-Nylon); dosage of cross-linker (0.75 mL); solvent (THF) and soaking-time (180 s). In order to check the result, a verification experiment under the optimal conditions was carried out. The resulting optimal MICM ($MICM_{opt}$) possessed higher adsorption capacity to EVO (47.39 μmol g^{-1}) compared to that of control $NICM_{opt}$ (15.29 μmol g^{-1}), resulting in a high imprinting factor of 3.099.

Interaction between template and functional monomer: In general, the recognition ability of imprinted polymer towards template molecule depends on the preservation of the pre-polymerized host-guest structure in a polymer matrix[15]. Therefore, it is important to investigate the interaction between template molecule and functional monomer in the pre-polymerization stage. The interaction between the basic template EVO and the acidic functional monomer MAA was estimated by UV spectrometry. Fig. 2 shows the UV spectra of EVO in the presence of MAA of seven different concentrations in THF determined against the control pure MAA solutions. It can be seen that the peak at 291 nm showed a blue shift along with a decreasing absorbance with the increase of MAA amount. Taking the structures of EVO and MAA into account, a supermolecular complex might be formed between EVO and MAA *via* hydrogen bond and/or static interaction. In order to explore more information about this complex, a theoretical analysis was carried out according to the literature[16].

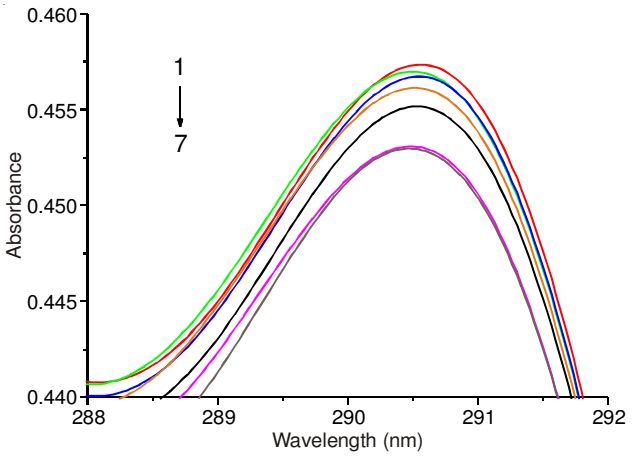

Fig. 2. UV spectra of EVO in the presence of MAA. Concentration of EVO: 0.04 mmol L^{-1}, concentrations of MAA for lines 1-7: 0, 0.04, 0.08, 0.12, 0.16, 0.20 and 0.24 mmol L^{-1}. Corresponding pure MAA solutions were used as blanks. MAA is the functional monomer methacrylate acid

The complex reaction of template (A) with functional monomer (B) can be described as the following equation:

$$A + nB = C \quad (1)$$

The association constant (K) of the reaction can be described as:

$$K = \frac{[C]}{[A][B]^n} \quad (2)$$

When the initial concentration of B (b_0) is greatly larger than that of A (a_0) and the absorption was determined at the wavelength where B cannot produce any absorption, the absorbance difference (ΔA), which is expressed as the absorption of the mixture with respect to the solution of A as blank, is

$$\frac{\Delta A}{b_0^n} = -K\Delta A + K\varepsilon a_0 l \quad (3)$$

$\Delta A/b_0^n$ was plotted *vs.* ΔA at 281 nm where MAA had no absorption. A good linear relationship with R of 0.9917 at n = 1 was obtained. The linear regression equation was calculated as $\Delta A/b_0 = 17.186 - 1.223 \times 10^4\ \Delta A$. The result indicated that a 1:1 complex was predominantly formed by EVO and MAA. The K value derived from the slope of regression equation was 1.223×10^4 mol^{-1} L, which indicated that EVO-MAA complex was stable enough to produce a good imprinting efficiency to EVO in the imprinting process.

SEM analysis: The surface morphology and the cross-section structure of the membranes were observed using SEM and the results are shown in Fig. 3. It can be seen that the surfaces of $MICM_{opt}$ (Fig. 3A) and $NICM_{opt}$ (Fig. 3B) are rougher than that of the base membrane CA-Nylon (Fig. 3C), suggesting that a thin layer of polymer was coated on CA-nylon. Furthermore, the images of cross-sections show that a large number of pores in the $NICM_{opt}$ and CA-Nylon membrane were blocked by some flocculent matters. By comparison, $MICM_{opt}$ possesses more cavities scattered on both the surface and cross-section than $NICM_{opt}$, which could be attributed to the effect of templates in preparing imprinted polymers. The porous structure formed in $MICM_{opt}$ after template extraction would reduce diffusion resistance and facilitate mass transfer. It is suggested that a high selectivity and flux can be expected in the case of $MICM_{opt}$.

Nitrogen adsorption: The N_2 adsorption/desorption isotherms of $MICM_{opt}$ and $NICM_{opt}$ are shown in Fig. 4. Both the membranes displayed the similar type IV isotherm, which is a character of mesoporous material[17]. However, pronounced differences existed in the adsorption/desorption isotherm of $MICM_{opt}$ (Fig. 4A) from that of $NICM_{opt}$ (Fig. 4B). The isotherm of $MICM_{opt}$ contained a hysteresis loop where desorption curve leveled off above the adsorption curve in the determined range. This implied that the $MICM_{opt}$ exhibited no shrinking when it subjected to increasing pressure at liquid N_2 temperature and those large imprinting pores in $MICM_{opt}$ had low swelling and solvent uptake[18]. This speculation was further verified by examining the distribution of pore size of $MICM_{opt}$ (Fig. 4A, insertion). It can be seen that two prominent peaks appeared in the pore distribution curve of $MICM_{opt}$, implying at least two types of pores were formed in the imprinting process.

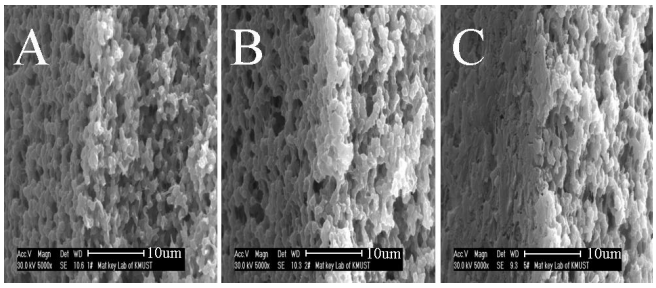

Fig. 3. Surface and cross-section SEM images of $MICM_{opt}$ (A), $NICM_{opt}$ (B) and CA-Nylon (C). $MICM_{opt}$ is the optimal molecularly imprinted composite membrane; $NICM_{opt}$ is the control non-imprinted composite membrane prepared in the absence of template molecule; and CA-Nylon is the supporting membrane

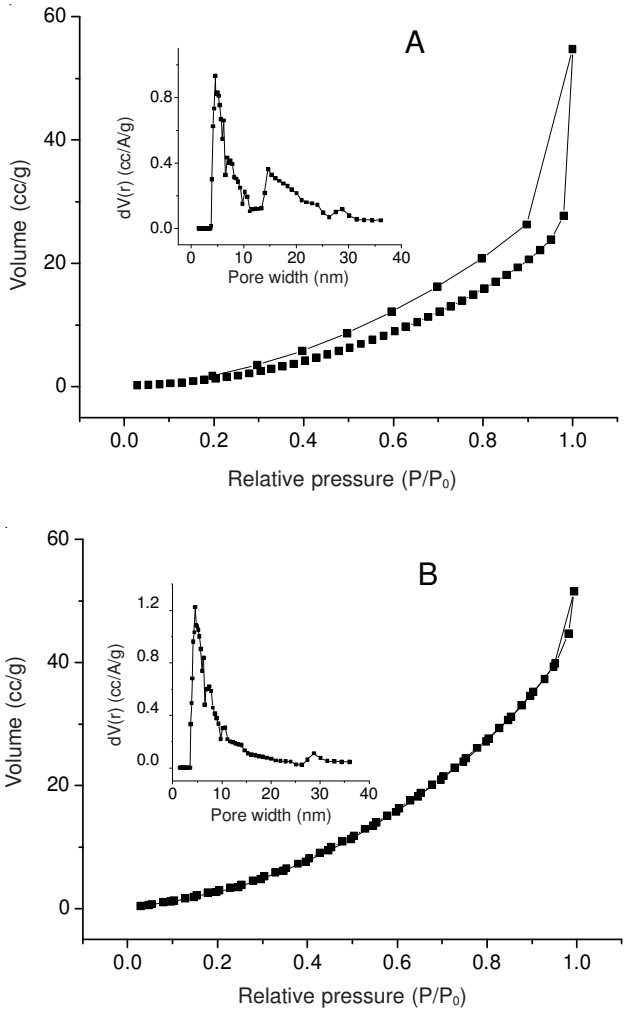

Fig. 4. Adsorption/desorption curve and pore size distribution (insertion) of $MICM_{opt}$ (A) and $NICM_{opt}$ (B). (A) Adsorption/desorption curve and pore size distribution (insertion) of $MICM_{opt}$. The isotherm of $MICM_{opt}$ contained a hysteresis loop where the above curve was desorption curve and the below was adsorption curve. The inserted figure is the distribution of pore sizes of $MICM_{opt}$. It revealed that at least two types of pores located in $MICM_{opt}$. (B) Adsorption/desorption curve and pore size distribution (insertion) of $NICM_{opt}$. Its adsorption/desorption curves were overlapped and only one peak is found on pores distribution curve. It revealed the structure of $NICM_{opt}$ was completely different from that of $MICM_{opt}$

The small pores (4.1 nm in diameter) were the result of the polymetharylate skeleton[18], while the larger ones (15 nm) might be attributed to the imprinted pores produced in imprinting process. Interestingly, the adsorption/desorption curve of $NICM_{opt}$ was overlapped and only one peak appeared on its pore distribution curve (Fig. 4B, insertion), revealing a structure difference from that of $MICM_{opt}$.

Permeation selectivity of membranes

Standard mixture analysis: For the membrane processing, the overall performance and practical feasibility depend on both permeability and selectivity[20]. The structural analogue RUT of EVO was used as a competitive compound to evaluate the permeation selectivity of $MICM_{opt}$. EVO/ RUT methanol mixture (60 mL, 0.10 mg mL^{-1} each) and pure methanol (60 mL) were poured into the two cells of an H-shape permeation device equipped with $MICM_{opt}$, $NICM_{opt}$ or the supporting membrane, respectively. Fig. 5 shows the permeating amounts of EVO and RUT through various membranes at 0-12 h.

As expected, $MICM_{opt}$ (Fig 5. A) showed higher selective permeability and transport ability to EVO in presence of the structural analogue RUT compared to $NICM_{opt}$ (Fig 5. B). Taking the penetration amounts at 12 h as a case, $MICM_{opt}$ (1.13 cm^2) can transport EVO 1.343 mg and RUT 0.841 mg, resulting in a relatively high selectivity factor (EVO/RUT) of up to 1.598, while the corresponding values for $NICM_{opt}$ were 0.7621 mg cm^{-2}, 0.6453 mg cm^{-2} and 1.181. These data demonstrate that $MICM_{opt}$ had a higher transport rate and selectivity to template than $NICM_{opt}$, which was consistent with the analysis results of SEM and N_2 adsorption analysis. The imprinting pores in $MICM_{opt}$ observed from the result of structural characterization are complementary to the template molecule in the size, shape and functional group arrangement and can preferably adsorb EVO from a complex system. According to the "gate effect" mechanism, a facilitated permeation is driven by preferential sorption to template molecules[20]. Therefore, EVO received better separation from RUT in the imprinted membrane system $MICM_{opt}$.

As a control, the transport ability of CA-Nylon supporting membrane was evaluated and the result is shown in Fig. 5C. CA-Nylon membrane yielded similar permeation selectivity to EVO as that of $NICM_{opt}$. The results indicate that the transport selectivity of EVO through $MICM_{opt}$ was mainly derived from the imprinting effect other than the inherent property of supporting membrane.

Analysis of real sample: In order to study the application potential of $MICM_{opt}$ in a real herb system, a MeOH crude extract of *E. rutaecarpa* was further analyzed in an H-shape permeation device. After the penetration test had been carried out for 12 h, 200 μL of diffusion solutions were taken out and analyzed by HPLC. The initial sample before penetration, as a control, was also analyzed. The concentrations of EVO and RUT in all sample solutions were summarized in Table-4. The ratio of mass concentration of EVO to RUT (EVO/RUT) was 9.283 in the initial solution and increased to 15.95 after the treatment by $MICM_{opt}$ barrier, indicating concentration of EVO was increased by 1.72 times. Under the same conditions, $NICM_{opt}$ only resulted in a slight increase of EVO/RUT. The results reveal that $MICM_{opt}$ could specifically recognize EVO from the real herb extract solution, suggesting a promising application potential of $MICM_{opt}$ in the enrichment of EVO from the crude extract solution of *E. rutaecarpa*.

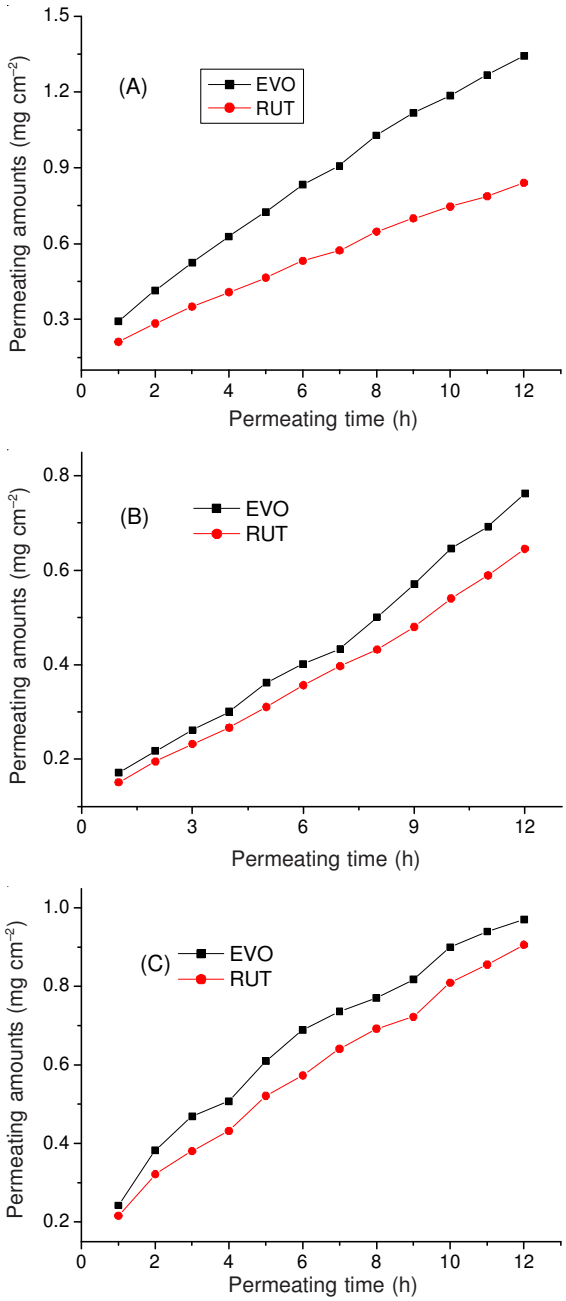

Fig. 5. Permeation curves of EVO and RUT through $MICM_{opt}$ (A), $NICM_{opt}$ (B) and the supporting membrane (C). The initial solution is 60 mL of EVO/RUT MeOH mixture (each as 0.10 mg mL^{-1}). (A) Illustrates the permeation curves of EVO and RUT through $MICM_{opt}$. It indicated that $MICM_{opt}$ could recognize EVO and gave a facilitated transport to EVO than RUT. (B) Illustrates the permeation curves of EVO and RUT through $NICM_{opt}$. It indicated that $MICM_{opt}$ could not effectively recognize EVO and gave almost equal transported amounts of both substrates. (C) Illustrates the permeation curves of EVO and RUT through the supporting membrane. It indicated similar permeation ability of the supporting membrane to that of $NICM_{opt}$

TABLE-4
CONCENTRATIONS OF SUBSTRATES IN *Evadia rutaecarpa* EXTRACT SOLUTION

Substrates	Initial extract solution	Penetration solution at 12 h	
		$MICM_{opt}$	$NICM_{opt}$
EVO (μg mL^{-1})	29.37	5.167	3.518
RUT (μg mL^{-1})	3.164	0.324	0.3153
EVO/RUT Ratio	9.283	15.95	11.16

Conclusion

In conclusion, the molecularly imprinted composite membranes (MICMs) prepared in the study can be a potential material in the separation and enrichment of evodiamine from the herb *E. rutaecarpa*.

ACKNOWLEDGEMENTS

This work was financially supported by the Natural Science Foundation of China (No. 20964005), as well as by a program for New Century Excellent Talents in University from MOE (No. NCET-08-0925) and a grant (No. 2009FL03) from Yunnan Tobacco Co., China.

REFERENCES

1. K.G. Shyu, S.K. Lin, C.C. Lee, E. Chen, L.C. Lin, B.W. Wang and S.C. Tsai, *Life Sci.*, **78**, 2234 (2006).
2. W.F. Chiou and C.F. Chen, *Eur. J. Pharmacol.*, **446**, 151 (2002).
3. H. Yu, Y.J. Tu, C. Zhang, X. Fan, X. Wang, Z.L. Wang and H.P. Liang, *Biochem. Biophys. Res. Commun.*, **402**, 94 (2010).
4. M. Ulbricht, *J. Chromatogr. B*, **804**, 113 (2004).
5. R.R. Chen, L. Qin, M. Jia, X.H. He and W.Y. Li, *J. Membr. Sci.*, **363**, 212 (2010).
6. S.G.D. Blanco, L. Ponato and E. Drioli, *Sep. Purif. Technol.*, **87**, 40 (2012).
7. G. Song, M.E. Kellam, D. Liang and M.D. Dolan, *J. Membr. Sci.*, **363**, 309 (2010).
8. I. Mijangos, F.N. Villoslada, A. Guerreiro, E. Piletska, I. Chianella, K. Karim, A. Turner and S. Piletsky, *Biosens. Bioelectron.*, **22**, 381 (2006).
9. S.H. Ma, H. Wang, Y. Wang, H.G. Bu and J.B Bai, *Renew. Energ.*, **36**, 709 (2001).
10. K.H. Lee, J. W. Yi, J.S. Park and G.J. Park, *Finite Elem. Anal. Des.*, **40**, 121 (2003).
11. E.L. Lawrence, R.J. Ball, R. Evans and R. Stevens, *J. Power Sources*, **110**, 125 (2002).
12. H.S. Andersson, J.G. Karlsson, S.A. Piletsky, A. Koch-Schmidt, K. Mosbach and I.A. Nicholls, *J. Chromatogr. A*, **848**, 39 (1999).
13. G.S. Wang, Q.E. Cao, Z.T. Ding, Y.G. Wang and M.H. Yang, *Helv. Chim. Acta*, **90**, 1179 (2007).
14. M.U. Ding, Q. Zi and H.L. Shu, *Computer-Aided Design*, **38**, 595 (2006).
15. T. Kusunoki and T. Kobayashi, *J. Appl. Polym. Sci.*, **117**, 565 (2010).
16. X.F. Zhu, Q.E. Cao, N.B. Hou and Z.T. Ding, *Anal. Chim. Acta*, **171**, 561 (2006).
17. P.P. Qi, J.C. Wang, L.D. Wang, Y. Li, J. Jin, F. Su, Y.Z. Tian and J. Chen, *Polymer*, **51**, 5417 (2010).
18. A.L. Hillberg, K.R. Brain and C.J. Allender, *J. Mol. Recognit.*, **22**, 223 (2009).
19. S.A. Piletsky, T.L. Panasyuk, E.V. Piletskaya, I.A. Nicholls and M. Ulbricht, *J. Membr. Sci.*, **157**, 263 (1999).
20. K. Hattori, M. Hiwatari, C. Iiyama, Y. Yoshimi, F. Kohori, K. Sakai and S.A. Piletsky, *J. Membr. Sci.*, **233**, 169 (2004).